Evidence of doping-dependent pairing symmetry in cuprate superconductors

N.-C. Yeh, C.-T. Chen, German Hammerl, Jochen Mannhart, Andreas Schmehl, Christof W. Schneider, Robert R. Schulz, S. Tajima, K. Yoshida, D. Garrigus, M. Strasik

Evidence of Doping-Dependent Pairing Symmetry in Cuprate Superconductors

N.-C. Yeh,[1] C.-T. Chen,[1] G. Hammerl,[2] J. Mannhart,[2] A. Schmehl,[2] C. W. Schneider,[2] R. R. Schulz,[2] S. Tajima,[3] K. Yoshida,[3] D. Garrigus,[4] and M. Strasik[4]

[1]*Department of Physics, California Institute of Technology, Pasadena, California 91125*
[2]*Center for Electronic Correlations and Magnetism, Institute of Physics, Augsburg University, D-86135 Augsburg, Germany*
[3]*Superconductivity Research Laboratory, International Superconductivity Technology Center, 1-10-13, Sinonome,*
Koto-ku, Tokyo, 135 Japan
[4]*Boeing Information, Space & Defense Systems, Renton, Washington 98055*
(Received 11 December 2000; published 3 August 2001)

Scanning tunneling spectroscopy studies reveal long-range spatial homogeneity and predominantly $d_{x^2-y^2}$-pairing spectral characteristics in under- and optimally doped $YBa_2Cu_3O_{7-\delta}$ superconductors, whereas STS on $YBa_2(Cu_{0.9934}Zn_{0.0026}Mg_{0.004})_3O_{6.9}$ exhibits *microscopic* spatial modulations and strong scattering near the Zn or Mg impurity sites, together with global suppression of the pairing potential. In contrast, in overdoped $(Y_{0.7}Ca_{0.3})Ba_2Cu_3O_{7-\delta}$, $(d_{x^2-y^2} + s)$-pairing symmetry is found, suggesting significant changes in the superconducting ground state at a critical doping value.

One of the most important issues associated with cuprate superconductors is the possible existence of a quantum critical point (QCP) near the optimal hole doping ($p_o \approx 0.16$ per CuO_2) in these doped Mott antiferromagnets [1–3]. Although nonmonotonic doping-dependent physical properties in the underdoped ($p < p_o$) and overdoped ($p > p_o$) regimes are suggestive of the presence of a QCP, an unambiguous proof would require identifying the relevant broken symmetry associated with a critical doping level p_c. Various theoretical studies [2,4] have investigated the dependence of the ground state of doped Mott antiferromagnets on the doping level and the strength of exchange and Coulomb interactions [2]. The relevant symmetries associated with the competing orders include the following: electromagnetic U(1), spin rotation-invariance SU(2), square lattice space group C_{4v}, and time-reversal symmetry $\mathcal{T}$ [2]. Experimentally, while the $d_{x^2-y^2}$ pairing symmetry is known to dominate in the optimally doped cuprates [5–9], possible doping-dependent pairing symmetry has been suggested [10]. In general, the doping dependence of the pairing symmetry and the issue of quantum criticality must be considered under the premise of spatial homogeneity in the pairing potential. The recent finding of nanoscale variations in the measured energy gap of $Bi_2Sr_2CaCu_2O_{8+x}$ (Bi-2212) [11] and the implication of macroscopic clusters in overdoped $La_{2-x}Sr_xCuO_4$ [12] present possible complications in unraveling the existence of a QCP.

A possible consequence of a QCP is the doping-dependent pseudogap phenomenon [13], which may represent a precursor for superconductivity in the cuprates [13]. Early experiments on the Bi-2212 system reported a measured energy gap $\Delta^*(p)$ that increased monotonically with decreasing p and was nearly independent of temperature [14–19]. However, the low-temperature spectra of the optimally doped and underdoped Bi-2212 appeared to consist of a sharp peak feature on top of a broad "hump." Recent bulk measurements on Bi-2212 mesas [20] demonstrated strong temperature dependence associated with the sharp peak, which vanished at the superconducting transition temperature T_c, while the hump feature persisted well above T_c. The coexistence of these two gaplike features in the superconducting state has been attributed to a different physical origin associated with each gap [20,21].

In this work, we address some of these issues via studies of the directional and spatially resolved quasiparticle tunneling spectra on the $YBa_2Cu_3O_{7-\delta}$ (YBCO) with a range of doping levels. The doping dependence of the pairing symmetry, pairing potential, and spatial homogeneity is derived from these studies.

The samples used in this investigation included three optimally doped YBCO single crystals with $T_c = 92.9 \pm 0.1$ K, three underdoped YBCO single crystals with $T_c = 60.0 \pm 1.5$ K, one underdoped YBCO c-axis film with $T_c = 85.0 \pm 1.0$ K, two overdoped $(Y_{0.7}Ca_{0.3})Ba_2Cu_3O_{7-\delta}$ (Ca-YBCO) c-axis films [22] with $T_c = 78.0 \pm 2.0$ K, and one optimally doped single crystal containing small concentrations of nonmagnetic impurities, $YBa_2(Cu_{0.9934}Zn_{0.0026}Mg_{0.004})_3O_{6.9}$ [(Zn,Mg)-YBCO], with $T_c = 82.0 \pm 1.5$ K [8,22]. The spectra of YBCO single crystals were taken primarily with the quasiparticles tunneling along three axes: the antinode axes {100} or {010}, the nodal axis {110}, and the c axis {001}; while those of the pure and Ca-YBCO films were taken along the c axis. All samples except (Zn,Mg)-YBCO are twinned. The surface was prepared by chemical etching [23,24], and samples were kept either in high-purity helium gas or under high vacuum at all times. Our surface preparation has the advantage of terminating the YBCO top surface at the CuO_2 plane by chemically passivating the layer while retaining the bulk properties of the constituent elements [23,24], thus yielding reproducible spectra for samples of the same

bulk stoichiometry, although direct constant-current mode atomic imaging of the chemically inert surface becomes difficult. For comparison, surfaces of vacuum-cleaved YBCO samples are found to terminate at the CuO-chain layer, which are prone to loss of oxygen and development of surface states [23,24]. For vacuum-cleaved Bi-2212, the surface typically terminates at the BiO layer.

Figure 1 illustrates representative tunneling conductance (dI_{NS}/dV) vs voltage (V) data with high spatial resolution for YBCO samples at 4.2 K: (a) optimally doped YBCO, with the average quasiparticle momentum $\vec{k} \parallel \{110\}$ and the tip scanning along $\{001\}$; (b) underdoped YBCO, with $\vec{k} \parallel \{100\}$ and scanning along $\{001\}$; and (c) Ca-YBCO, with $\vec{k} \parallel \{001\}$ and scanning along $\{100\}$. The normalized (dI_{NS}/dV) vs V spectra of under- and (Zn,Mg)-doped YBCO for $\vec{k} \parallel \{100\}$ are shown in the inset of Fig. 1(b), and those of underdoped, (Zn,Mg)-doped, and Ca-doped YBCO for $\vec{k} \parallel \{001\}$ are illustrated in
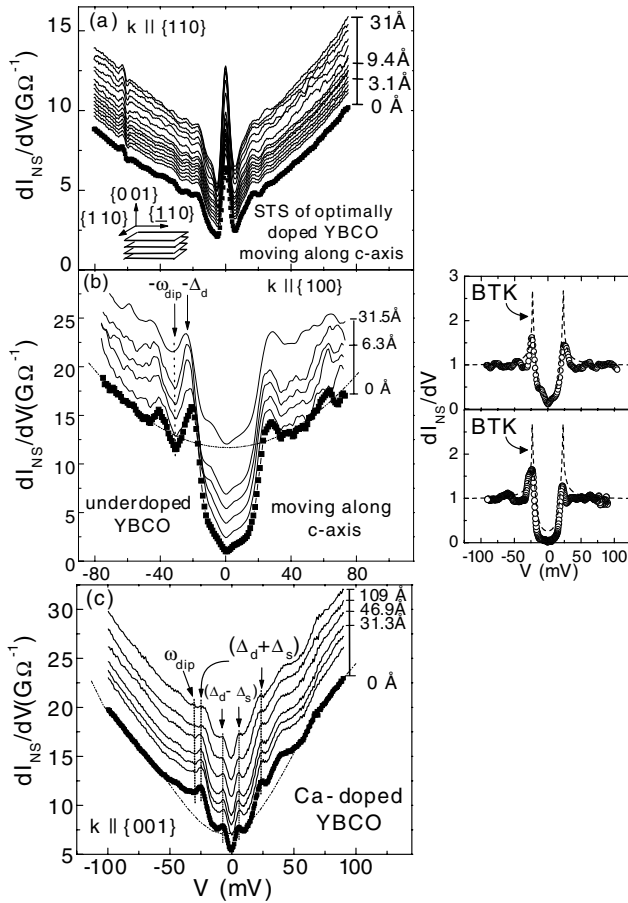

FIG. 1. Spatially resolved (dI_{NS}/dV) vs (V) spectra at 4.2 K: (a) Optimally doped YBCO. (b) Underdoped YBCO. Panels: normalized $\{100\}$ spectra of an underdoped YBCO (upper panel) and (Zn,Mg)-YBCO (lower panel) together with a BTK fitting curve (dashed line). (c) Ca-YBCO: The tunneling cone [7–9] of all spectra ranges from $(\pi/12)$ to $(\pi/8)$. For the BTK analysis, each set of the data was normalized relative to the polynomial fit to the high-voltage background conductance, as shown in (b) and (c) by the dashed-dotted curve.

Fig. 2(a). To verify the spatial resolution, we also performed (dI_{NS}/dV) mapping of an optimally doped single crystal at a constant bias voltage of $V \approx (\Delta_d/e)$ with tip scanning along $\{001\}$ and $\vec{k} \parallel \{100\}$. Periodic conductance modulations consistent with the known atomic layer separations in YBCO were resolved. Independent imaging on NbSe$_2$ also confirmed atomic spatial resolution.

For the optimally doped and underdoped YBCO, the STS exhibited long-range (~ 100 nm) spatial homogeneity and strong directionality, showing a zero-bias conductance peak (ZBCP) for $\vec{k} \parallel \{110\}$ [7–9,25,26] [Fig. 1(a)]; nearly "U-shape" gap features around the zero bias for $\vec{k} \parallel \{100\}$, [Fig. 1(b)]; and "V-shape" features for $\vec{k} \parallel \{001\}$, [Fig. 2(a)]. By taking into account a finite transverse momentum distribution for the incident quasiparticles relative to the normal of the crystalline plane (i.e., by considering a finite "tunneling cone," parametrized as β with a typical value ranging from 15° to 22.5° [9]), the primary features and the directionality of the spectra of all optimally doped and underdoped YBCO samples were consistent with the generalized Blonder-Tinkham-Klapwijk (BTK) theory by Hu [25], Kashiwaya and Tanaka [26] for $d_{x^2-y^2}$ pairing [7–9,25,26].

For the Ca-doped YBCO epitaxial films, *macroscopic* spatial variation in the STS at a length scale of ~ 50 nm was observed, which correlated with the dimension of the growth islands according to images of atomic force microscopy [22], while the STS within each island were spatially homogeneous, as exemplified in Fig. 1(c). The spatial modulation of STS may be the result of macroscopic phase segregation, similar to the finding in overdoped LSCO [12]. Furthermore, the STS of Ca-YBCO exhibited long-range and symmetric "subgap peaks," [see Figs. 1(c) and 2(a)], which differed from the spectral contributions of local disorder (such as oxygen vacancies), the latter generally appeared as short-range and asymmetric "humps" in the spectra. These spectra were in good agreement with the $(d_{x^2-y^2} + s)$ pairing symmetry according to the generalized BTK analysis [7–9,25,26], with a pairing potential $\Delta_k = \Delta_d \cos 2\theta_k + \Delta_s$, where θ_k is the angle of $\vec{k}$ relative to $\{100\}$. We obtained two typical sets of spectra with $\Delta_d = 17$ meV and $\Delta_s = 9$ meV for data in Fig. 1(c), and $\Delta_d = 13$ meV and $\Delta_s = 6$ meV for the other set of spectra given elsewhere [7]. On the other hand, $d_{x^2-y^2}$ pairing symmetry was confirmed on the optimally doped and underdoped YBCO c axis epitaxial films prepared by two research groups, as exemplified in the inset of Fig. 2(a) for a YBCO film with $T_c = 85.0 \pm 1.0$ K. For clarity, we depict the calculated c axis tunneling spectra in Fig. 2(b). Thus, under the premise that the spectra are spatially homogeneous well beyond the coherence length and mean free path, we suggest that *the long-range and symmetric subgap peaks in overdoped YBCO represent supporting evidence for doping-induced variations in the pairing symmetry.* The substantial s-pairing component ($>20\%$) may also contribute to the significant enhancement in the
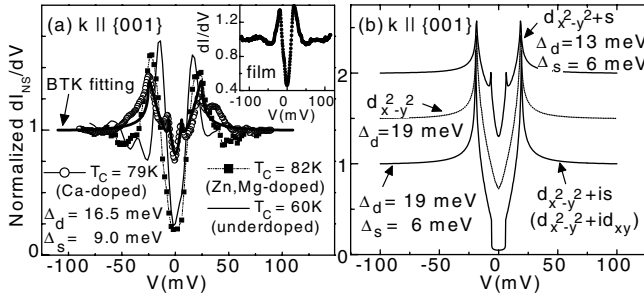
FIG. 2.   (a) Normalized c axis tunneling spectra of one under-doped, one (Zn,Mg)-doped, and one Ca-YBCO, together with a BTK fitting curve to the Ca-YBCO spectrum (the thick solid line). Inset: c-axis spectrum of an underdoped YBCO film. (b) Calculated spectra for different pairing symmetries.

critical current of bi-crystal Josephson junctions and poly-crystalline samples based on the Ca-YBCO [22].

The maximum value of the d-wave gap, Δ_d, appeared to be nonmonotonic with the doping level p [Fig. 3(a)], whereas the ratio $(2\Delta_d/k_BT_c)$ increased with decreasing doping, from ~7.8 for $p \approx 0.09$ to ~4.5 for $p \approx 0.22$, as illustrated in Fig. 3(b). On the other hand, experiments on Bi-2212 found an averaged gap Δ^* that scaled with the pseudogap temperature T^*, $2\Delta^* \sim 6.6k_BT^*$ [14–19], and that Δ^* increased with decreasing p [14–19]. We speculate that the superlattice and charge-density-wave modulations of the BiO layers in Bi-2212 may have complicated the quasiparticle spectra [14–21]. Furthermore, the tendency of random oxygen distribution in Bi-2212, as opposed to the generally ordered oxygen distribution in YBCO, may be responsible for the nanoscale variations in Δ^* of Bi-2212, ranging from ~15 to ~70 meV over a few nanometers [11].

Although the generalized BTK analysis was suitable for deriving the pairing potential and the primary spectral characteristics, it could not account for the "satellite features" associated with many-body interactions [27] in all YBCO spectra. In Bi-2212, the spectral "dip/hump" features were widely observed [14–19] and attributed to quasiparticle damping via interactions with collective spin fluctuations [27,28]. In the strong coupling limit, the spectral dip is expected to appear at the energy $\omega_{dip} = \Delta + \Omega_{res}$, where Δ is the measured gap, and Ω_{res} is associated with the resonance of collective spin excitations [27,28]. Defining Ω_{res} as the energy difference between the primary peak (Δ) and the dip (ω_{dip}) in the spectra [28], as indicated by the solid arrows in Figs. 1(b) and 1(c), we found that Ω_{res} in YBCO decreased with decreasing p, as shown in the inset of Fig. 3(a).

In the (Zn,Mg)-YBCO single crystal, *microscopic* spatial variations were observed. Two types of impurity scattering spectra were found. One was associated with a resonant scattering at (-10 ± 2) meV, as shown in Fig. 4, the other at (4 ± 2) meV. Assuming the position where a local maximum intensity of a resonant peak occurred as an impurity site, we found that the peak persisted over several lattice constants for displacement along either {100} or
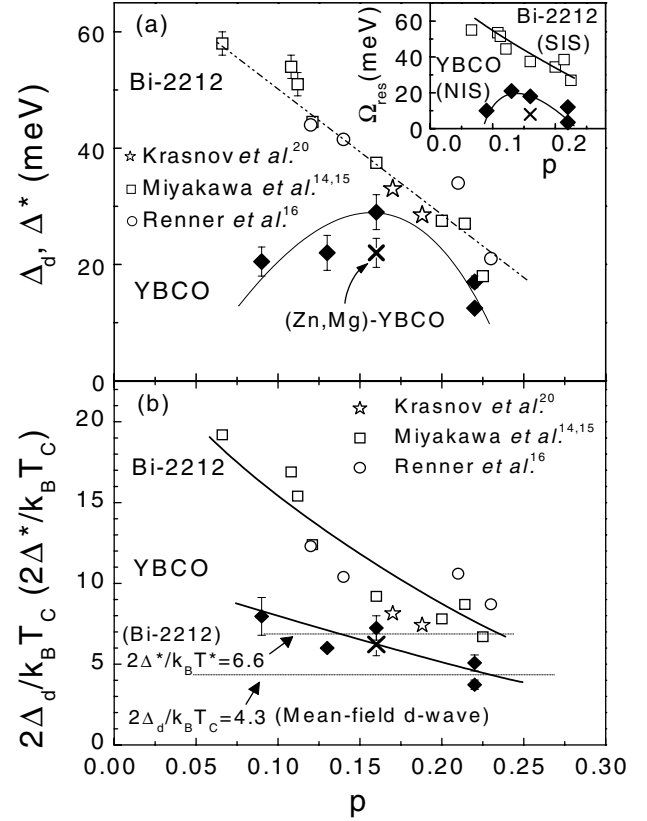

FIG. 3.   (a) Comparison of $\Delta_d(p)$ in YBCO with $\Delta^*(p)$ in Bi-2212. The doping level p is determined from the formula $T_c = T_{c,max}[1 - 82.6(p - 0.16)^2]$ [7] with $T_{c,max} = 93.0$ K. Inset: Comparison of $\Omega_{res}(p)$ for YBCO and Bi-2212. (b) Doping-dependent $(2\Delta_d/k_BT_c)$ for YBCO and $(2\Delta^*/k_BT_c)$ for Bi-2212. The error bar associated with each doping level of YBCO covers the range of Δ_d (or Ω_{res}) obtained from all spectra and the uncertainties of the BTK fitting.

{010}, and the peak intensity decreased rapidly within the Fermi wavelength, as shown in the inset of Fig. 4. Eventually the usual spectrum was recovered at about two coherence lengths (~3 nm) from an impurity site, similar to Zn-doped Bi-2212 [29]. For displacement along other directions, the spectral features became more complicated [30]. Our data have confirmed that the spinless impurities such as Zn^{2+} and Mg^{2+} are strong pair breakers [29–38]. Furthermore, the magnitude of the global Δ_d and Ω_{res} in (Zn,Mg)-YBCO both became smaller than those of the optimally doped YBCO, as shown in Fig. 3(a). The strong suppression of Ω_{res} suggests that the spinless impurity-induced moments may be responsible for the suppression of collective spin excitations [38]. The single resonance peak at the spinless impurity site is also in contrast to the predicted double peaks (at $\pm E_0$) at the impurity site had the $\mathcal{T}$ symmetry been broken due to a complex pairing symmetry of either $(d_{x^2-y^2} + id_{xy})$ or $(d_{x^2-y^2} + is)$ [35].

In the context of quantum criticality, our data of doping-dependent pairing symmetry is suggestive of a QCP with broken C_{4v} symmetry. However, a small s-pairing component beyond the resolution of our STS might exist in the under- and optimally doped YBCO due to the crystalline
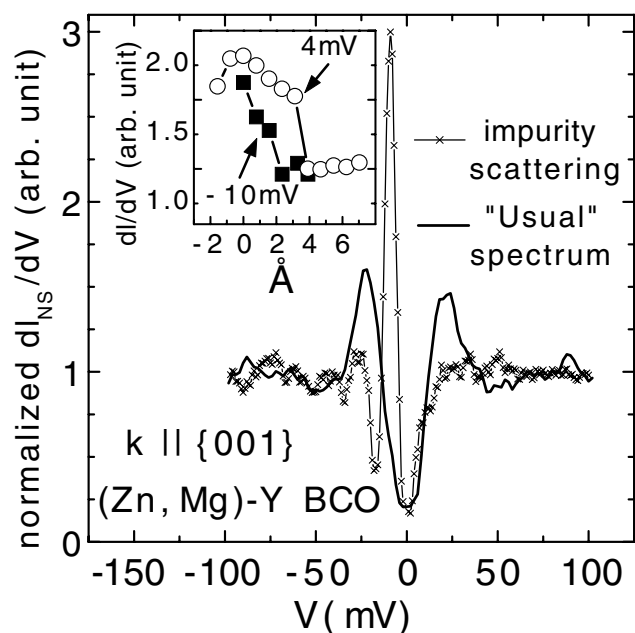
FIG. 4. {001} tunneling spectrum of (Zn,Mg)-YBCO at a spinless impurity site and a usual spectrum away from any impurity. Two types of impurity scattering were observed: one at (-10 ± 2) meV, the other at (4 ± 2) meV. Inset: Rapidly decreasing intensity of the scattering peaks are shown for displacement along {010} from an impurity site.

orthorhombicity, which would imply that no obvious broken symmetry had taken place. For comparison, no doping dependence in the pairing symmetry has ever been observed in tetragonal Bi-2212. On the other hand, the absence of either $(d_{x^2-y^2} + id_{xy})$ or $(d_{x^2-y^2} + is)$ pairing does not rule out the possibility of broken $\mathcal{T}$ symmetry at a QCP, because certain broken $\mathcal{T}$ symmetry states, such as the staggered flux [3,39] and the circulating current phase [1], cannot be detected directly by tunneling spectra. However, to date no universal broken symmetry associated with a QCP can be identified for all cuprate superconductors.

In summary, we have demonstrated long-range spatial homogeneity in the quasiparticle tunneling spectra of YBCO samples with a range of doping levels. In contrast, STS of the (Zn,Mg)-YBCO exhibit strong pair-breaking effects near the Zn and Mg impurities. The quasiparticle spectral characteristics and the impurity scattering effects in optimally doped and underdoped YBCO are consistent with predominantly $d_{x^2-y^2}$ ($>95\%$) pairing symmetry, whereas those of the overdoped Ca-YBCO exhibit $(d_{x^2-y^2} + s)$ pairing symmetry with a significant s component ($>20\%$).

[1] C. M. Varma, Phys. Rev. B **55**, 14 554 (1997).
[2] M. Vojta, Y. Zhang, and S. Sachdev, Phys. Rev. B **62**, 6721 (2000), and references therein.
[3] S. Chakravarty and H. Y. Kee, Phys. Rev. B **61**, 14 821 (2000).
[4] D. H. Lee, Phys. Rev. Lett. **84**, 2694 (2000).
[5] C. C. Tsuei and J. R. Kirtley, Rev. Mod. Phys. **72**, 969 (2000), and references therein.
[6] D. J. Van Harlingen, Rev. Mod. Phys. **67**, 515 (1995).
[7] N.-C. Yeh *et al.,* cond-mat/0103205, 2001 [Physica (Amsterdam) C (to be published)].
[8] N.-C. Yeh *et al.,* Physica (Amsterdam) **341C–348C**, 1639 (2000).
[9] J. Y. T. Wei, N.-C. Yeh, D. F. Garrigus, and M. Strasik, Phys. Rev. Lett. **81**, 2542 (1998).
[10] G. Deutscher, Nature (London) **397**, 410 (1999).
[11] S. H. Pan and J. C. Davis (private communications).
[12] H. H. Wen, X. H. Chen, W. L. Yang, and Z. X. Zhao, Phys. Rev. Lett. **85**, 2805 (2000).
[13] T. Timusk and B. Statt, Rep. Prog. Phys. **62**, 61 (1999).
[14] N. Miyakawa *et al.,* Phys. Rev. Lett. **83**, 1018 (1999).
[15] N. Miyakawa *et al.,* Phys. Rev. Lett. **80**, 157 (1998).
[16] C. Renner *et al.,* Phys. Rev. Lett. **80**, 149 (1998).
[17] M. R. Norman and H. Ding, Phys. Rev. B **57**, R11 089 (1998), and references therein.
[18] A. V. Fedorov *et al.,* Phys. Rev. Lett. **82**, 2179 (1999).
[19] Z. X. Shen and D. S. Dessau, Phys. Rep. **253**, 2 (1995).
[20] V. M. Krasnov *et al.,* Phys. Rev. Lett. **84**, 5860 (2000).
[21] Y. Bang and H. Y. Choi, Phys. Rev. B **62**, 11 763 (2000).
[22] C. W. Schneider *et al.,* Appl. Phys. Lett. **75**, 850 (1999).
[23] R. P. Vasquez, B. D. Hunt, and M. C. Foote, Appl. Phys. Lett. **54**, 2373 (1989).
[24] R. P. Vasquez, M. C. Foote, and B. D. Hunt, Appl. Phys. Lett. **55**, 1801 (1989).
[25] C. R. Hu, Phys. Rev. Lett. **72**, 1526 (1994).
[26] Y. Tanaka and S. Kashiwaya, Phys. Rev. Lett. **74**, 3451 (1995).
[27] C. L. Wu, C. Y. Mou, and D. Chang, Phys. Rev. B **63**, 172 503 (2001).
[28] A. V. Chubukov, N. Gemelke, and A. Abanov, Phys. Rev. B **61**, R6467 (2000).
[29] S. H. Pan *et al.,* Nature (London) **403**, 746 (2000).
[30] C. T. Chen, N. C. Yeh, K. Yoshida, and S. Tajima (to be published).
[31] H. F. Fong *et al.,* Nature (London) **398**, 588 (1999).
[32] J. Figueras, T. Puig, A. E. Carrillo, and X. Obradors, Supercond. Sci. Technol. **13**, 1067 (2000).
[33] A. V. Balatsky, M. I. Salkola, and A. Rosengren, Phys. Rev. B **51**, 15 547 (1995).
[34] M. E. Flatte and J. M. Byers, Phys. Rev. Lett. **80**, 4546 (1998).
[35] M. I. Salkola and J. R. Schrieffer, Phys. Rev. B **58**, R5952 (1998).
[36] Y. Sidis *et al.,* Phys. Rev. Lett. **84**, 5900 (2000).
[37] S. Haas and K. Maki, Phys. Rev. Lett. **85**, 2172 (2000).
[38] A. Polkovnikov, S. Sachdev, and M. Vojta, Phys. Rev. Lett. **86**, 296 (2001).
[39] I. Affleck, Z. Zou, T. Hsu, and P. W. Anderson, Phys. Rev. B **38**, 745 (1988).